ACS Synthetic Biology
Cite This: ACS Synth. Biol. 2020, 9, 10−18
Letter
pubs.acs.org/synthbio

Point-of-Use Detection of Environmental Fluoride *via* a Cell-Free Riboswitch-Based Biosensor

Walter Thavarajah,[†,§,∥] Adam D. Silverman,[†,§,∥] Matthew S. Verosloff,[‡,§,∥] Nancy Kelley-Loughnane,[⊥] Michael C. Jewett,[†,§] and Julius B. Lucks*[,†,§,∥]

[†]Department of Chemical and Biological Engineering, Northwestern University, 2145 Sheridan Road, Evanston, Illinois 60208, United States

[‡]Interdisciplinary Biological Sciences Graduate Program, Northwestern University, 2204 Tech Drive, Evanston, Illinois 60208, United States

[§]Center for Synthetic Biology, Northwestern University, 2145 Sheridan Road, Evanston, Illinois 60208, United States

[∥]Center for Water Research, Northwestern University, 2145 Sheridan Road, Evanston, Illinois 60208, United States

[⊥]Materials and Manufacturing Directorate, Air Force Research Laboratory, Wright-Patterson Air Force Base, Ohio 45433, United States

Supporting Information

ABSTRACT: Advances in biosensor engineering have enabled the design of programmable molecular systems to detect a range of pathogens, nucleic acids, and chemicals. Here, we engineer and field-test a biosensor for fluoride, a major groundwater contaminant of global concern. The sensor consists of a cell-free system containing a DNA template that encodes a fluoride-responsive riboswitch regulating genes that produce a fluorescent or colorimetric output. Individual reactions can be lyophilized for long-term storage and detect fluoride at levels above 2 ppm, the Environmental Protection Agency's most stringent regulatory standard, in both laboratory and field conditions. Through onsite detection of fluoride in a real-world water source, this work provides a critical proof-of-principle for the future engineering of riboswitches and other biosensors to address challenges for global health and the environment.

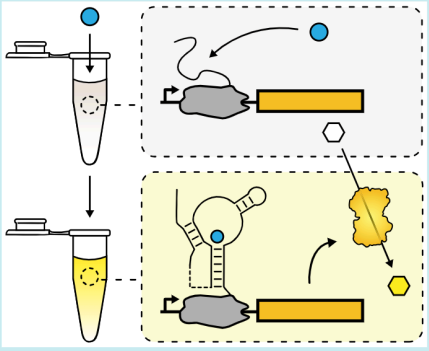

KEYWORDS: *riboswitches, biosensor, cell-free systems, diagnostics, water quality, field use*

Safe drinking water availability is an important contributor to public welfare.[1] However, safe water sources are not available to a large portion of the globe, with an estimated 3 billion people using water from either an unsafe source or a source with significant sanitary risks.[2] One particularly dangerous contaminant is fluoride, which leaches into groundwater from natural sources. Long-term exposure to fluoride concentrations above 2 ppm can cause dental and skeletal fluorosis, heavily burdening communities in resource-limited settings.[3] Though large-scale remediation strategies are available, they are resource-intensive and difficult to deploy.[3,4] This problem is compounded by the reliance of gold-standard sensing methods on expensive analytical equipment, making detection difficult in areas with the greatest need.[4] While many emerging fluorescent and colorimetric chemical fluoride sensors exist, these either require supplementary imaging equipment or utilize toxic organic solvents, hampering their use in real-world conditions.[5] To facilitate targeted remediation and empower affected individuals, there is a pressing need for a more practical, rapid, and field-deployable solution to monitor the presence of fluoride in water.

Because they can be lyophilized and rehydrated on-demand, cell-free expression (CFE) systems have recently become a promising platform for field-deployable molecular diagnostics.[6−9] These systems typically consist of cellular gene expression machinery along with the required buffers, energy sources and cofactors necessary to support gene expression from added DNA templates.[10] Unlike whole cells, cell-free platforms offer an open, easily tunable reaction environment, expediting the design process for genetically encoded programs.[10] Furthermore, they circumvent the analyte toxicity, host mutation, and biocontainment concerns limiting cellular sensors.[11]

We sought to leverage the advantages of cell-free biosensing platforms to create a new approach for monitoring for the presence of fluoride in water using a fluoride-responsive riboswitch that regulates the expression of the CrcB fluoride efflux pump in *Bacillus cereus*.[12] By configuring the *B. cereus crcB* fluoride riboswitch to control the transcription of downstream reporter genes,[13] we show that a cell-free gene

Received: August 27, 2019
Published: December 12, 2019

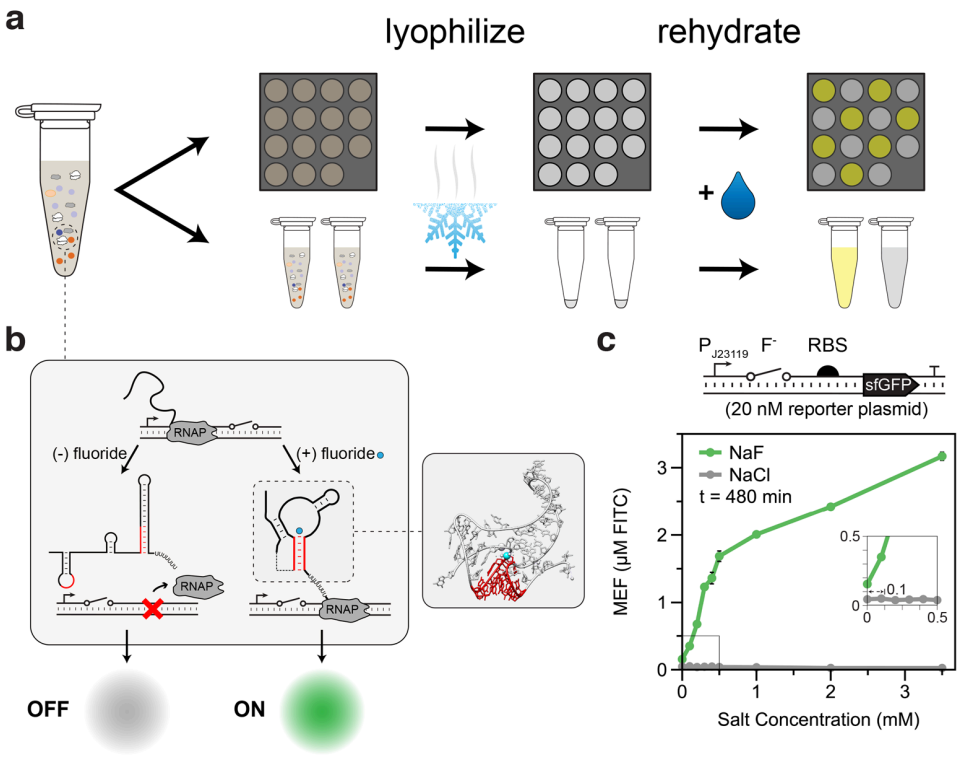

Figure 1. Cell-free fluoride biosensor engineering strategy. (a) Schematic for lyophilization of a cell-free reaction in tubes or on paper disks. Rehydration with a water sample allows the designed biosensing reaction to proceed to yield a detectable signal. (b) Schematic for fluoride riboswitch-mediated transcriptional regulation in cell-free extract. The riboswitch folds cotranscriptionally into one of two mutually exclusive states, depending on the presence of fluoride. In the absence of fluoride, the riboswitch folds into a terminating hairpin, precluding downstream gene expression. Fluoride binding stabilizes a pseudoknot structure (red paired region, inset from PDB: 4ENC) that sequesters the terminator and enables the expression of downstream reporter genes. (c) Schematic of a cell-free fluoride biosensor, consisting of a DNA template encoding the fluoride riboswitch controlling the expression of sfGFP. Eight-hour end point fluorescence measurements for reactions containing NaF (dark green) or NaCl (gray) are shown below. Error bars represent one standard deviation from three technical replicates.

expression system can activate both protein and RNA reporter expression in the presence of fluoride. With an enzymatic colorimetric reporter, we demonstrate detection of fluoride concentrations at the Environmental Protection Agency (EPA) Secondary Maximum Contaminant Level of 2 ppm.[14] Notably, these cell-free biosensors showed more accurate sensing with a lower limit of detection than several tested commercially available consumer fluoride testing kits. We also demonstrate that our fluoride biosensor can be lyophilized for long-term storage and distribution, allowing us to detect fluoride in unprocessed groundwater obtained and tested onsite in Costa Rica. This work exemplifies the potential of riboswitches as practical biosensing tools and helps lay the foundation for utilizing cell-free biosensing systems in rapid and field-deployable water quality diagnostics to address pressing challenges in global health.

RESULTS

Fluoride Riboswitch Control of Reporter Expression in Cell-Free Reactions. Our point-of-use diagnostic consists of a cell-free system containing a fluoride biosensor DNA template that can be lyophilized and stored. Rehydration activates the biosensor, which encodes the fluoride riboswitch and a reporter gene that produces a detectable output if fluoride is present (Figure 1a,b). As a starting point, we sought to characterize the regulatory activity of the *B. cereus crcB* riboswitch in the cell-free reaction environment. Previous characterization of the riboswitch's cotranscriptional folding mechanism (Figure 1b) confirmed that it functions with *E. coli* RNA polymerase,[13] allowing us to use it in *E. coli* cell-free extract. We therefore constructed a reporter plasmid containing the riboswitch sequence followed by a strong ribosome binding site (RBS) and the coding sequence of the reporter protein superfolder green fluorescent protein (sfGFP), all placed downstream of a constitutive *E. coli* σ^{70} promoter (all plasmid details in Supplemental Table S1).

After optimizing the level of Mg^{2+} within the reaction conditions for riboswitch performance (Supplemental Figure S1), we determined the fluoride sensor's dose–response to fluoride by titrating across a range of NaF concentrations. All tested conditions caused a measurable increase in expression over the OFF state, with activation seen at NaF concentrations as low as 0.1 mM (Figure 1c, green line and inset). This threshold is important, since 0.1 mM NaF is equivalent to the EPA's 2 ppm secondary maximum contaminant level for fluoride in drinking water, its most stringent risk threshold.[14] However, because the signal-to-noise ratio at 0.1 mM NaF is below 3, we estimated the reliable lower limit of detection to be 0.2 mM NaF. Importantly, the system also has low leak—we observed minimal activation of gene expression in the absence of NaF. Titration of identical concentrations of NaCl showed no increase in expression at any condition, demonstrating that the riboswitch is highly specific for fluoride (Figure 1c, gray line). This result corroborates a previous and

DOI: 10.1021/acssynbio.9b00347
ACS Synth. Biol. 2020, 9, 10−18

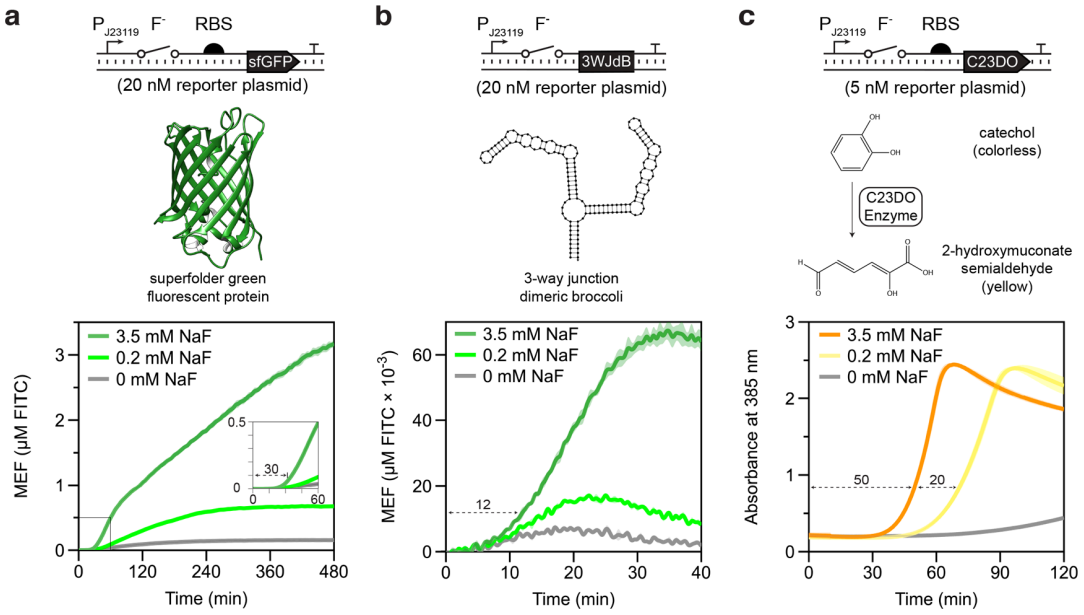

Figure 2. Riboswitch modularity allows fluorescent protein, RNA aptamer, and enzymatic colorimetric reporter outputs. Biosensor DNA template layouts and concentrations shown above reporter information and characterization data for that reporter. (a) Superfolder GFP (sfGFP) reporter (structure from PDB: 2B3P). Time course of fluorescence in the presence of 3.5 mM NaF (dark green), 0.2 mM NaF (light green), or 0 mM NaF (gray). (b) Three-way junction dimeric Broccoli reporter (structure predicted from NUPACK[15]). Time course of fluorescence in the presence of 3.5 mM NaF (dark green), 0.2 mM NaF (light green), and 0 mM NaF (gray). (c) Catechol (2,3)-dioxygenase (C23DO) reporter. Reaction scheme shows the cleavage of the colorless catechol molecule into the yellow 2-hydroxymuconate semialdehyde. Time course of absorbance at 385 nm in the presence of 3.5 mM NaF (orange), 0.2 mM NaF (yellow), and 0 mM NaF (gray). For each plot, trajectories represent average and error shading represents one standard deviation from three technical replicates. (a) and (b) are reported in mean equivalent fluorescence (MEF).

more extensive characterization in *E. coli* of the switch's specificity for fluoride.[12] Thus, without any optimization of riboswitch structure or function, the sensor can discriminate health-relevant concentrations of fluoride dosed into laboratory water samples.

Changing Reporters to Tune Sensor Speed and Detection Threshold. Biosensor field deployment requires an output that can be quickly read with minimal supplemental equipment.[16] Using the maximally activating fluoride concentration (3.5 mM), reactions achieved measurable signal above the no-fluoride OFF state in 30 min at 30 °C, with overall 20-fold activation relative to the no-fluoride condition at the end of the 8-h experiment (Figure 2a). Despite this, the sensor's ON state was not distinguishable by eye for several hours even after excitation with a blue LED, presenting the need for a faster reporter.

We hypothesized that we could accelerate the sensor's response with a 3-way junction dimeric Broccoli (3WJdB)[17] reporter, an RNA aptamer that activates fluorescence of its DFHBI-1T ligand upon transcription, eliminating delays caused by translation. At all tested NaF concentrations, 3WJdB produced a signal detectable over background within 12 min at 30 °C (Figure 2b), more than twice as fast as could be achieved with sfGFP (Figure 2a). Interestingly, this result also confirms that the fluoride riboswitch is compatible with RNA reporters, despite the potential for misfolding with the upstream riboswitch sequence. However, despite the improvement in speed, exchanging sfGFP for 3WJdB resulted in a 50-fold reduction in the sensor's fluorescent output at the maximally activating tested condition. Thus, although the RNA-level output is preferable for its speed relative to the sfGFP output if a plate reader is accessible, it is not bright enough to use for field deployment.

As an alternative to a fluorescent output, we used the colorimetric enzyme catechol (2,3)-dioxygenase (C23DO) as a reporter. C23DO has previously been used in genetically encoded biosensors for plant viruses[18] and produces a visible reporter output by oxidizing its colorless catechol substrate to the yellow-colored 2-hydroxymuconate semialdehyde.[19] This color change allows gene expression to be read out either by light absorbance at 385 nm on a plate reader or by the appearance of a yellow color, visible to the naked eye. All tested fluoride concentrations produced a visible output within 70 min at 30 °C, which we empirically defined as an absorbance of 0.8 based on our previous observations (Figure 2c).[18] Notably, there was only a 20 min time separation between the minimally and maximally activating conditions, highlighting the ability of enzymatic reporters to quickly amplify weak signals. Consistent with previous uses of C23DO as a reporter in a cell-free reaction,[19] we observed a decay in the absorbance signal after it reached peak activation, possibly due to 2-hydroxymuconate semialdehyde degradation. This effect does not compromise sensor robustness because differences in activation for an enzymatic reporter are determined by differences in time to observable signal rather than final signal magnitude, which is determined by the amount of substrate supplied. One disadvantage of this strategy is that activation time does not linearly correlate with fluoride concentration, limiting the sensor to only supplying a binary presence/absence result within a specified time window.[16] Despite this, the sensor's sensitivity and low leak make this presence/absence result diagnostically informative, which combined with the advantages of an easily visualized output

DOI: 10.1021/acssynbio.9b00347
ACS Synth. Biol. 2020, 9, 10−18

and reasonable time to detection made C23DO our reporter of choice for a field-deployable diagnostic.

Reaction Tuning and Lyophilization toward Biosensor Field Deployment. We next took steps to optimize our sensor to detect fluoride near the EPA's secondary maximum contaminant limit of 2 ppm (100 μM). We obtained a robust ON signal with our original design, but the sensor began to leak without fluoride after 90 min (Figure 2c, gray line), complicating detection for trace amounts of fluoride. We attempted to mitigate this problem by reducing the amount of reporter DNA supplied to the reaction from 5 nM to 3 nM to diminish the sensor's output. In doing so, we completely suppressed leak while detecting 100 μM NaF over background (Figure 3a), but at the cost of significantly delaying activation. We could detect as low as 50 μM NaF over background in this leakless sensor, but only during an extended incubation that did not reach a visually detectable threshold within 6 h.

To solve this dilemma and maintain a practical incubation time, we sought a strategy whereby tests could be interpreted as "ON" only if the yellow color appeared within some externally specified time window. Under these constraints, sensor leak is not a problem as long as the difference in time scale between the ON and OFF state is suitably longer than the test time. To implement this strategy, we increased biosensor DNA concentration to 10 nM and also increased the temperature of the CFE reaction to 37 °C. Under these conditions, activation by 100 μM NaF resulted in a clear color change in 60 min with no visible leak in the OFF condition (Figure 3b, Supplemental Figure S2). The same conditions using 3 nM DNA template resulted in no color change within 60 min. This result highlights an appreciable advantage afforded by the open reaction environment of cell-free systems: the sensor's limit of detection can be tuned simply by manipulating the reaction time and the DNA concentration of the biosensor.

Recent work demonstrates that CFE reactions can be lyophilized and rehydrated when needed for on-demand biomanufacturing, nucleic acid detection, and educational activities.[6,7,20,21] To expand these applications to point-of-use small molecule detection, we next aimed to demonstrate that fluoride biosensor reactions maintain functionality after being lyophilized. We measured the impact of lyophilization on fluoride detection by lyophilizing reactions containing 10 nM C23DO reporter plasmid overnight. The reactions were then rehydrated with laboratory grade Milli-Q water (Figure 3c, top) or water containing 1 mM NaF (Figure 3c, bottom) and incubated at 37 °C. Time-lapse photography shows visible activation within 60 min in the 1 mM NaF condition with no leak observed within 100 min in the no-fluoride condition (Supplemental Video S1). This finding, consistent with other recent reports from lyophilized cell-free systems,[6,7,20,21] indicates that sensing by the fluoride riboswitch in CFE reactions is not disrupted by the lyophilization process.

We also tested the viability of lyophilized reactions stored over longer periods of time. After lyophilization, reaction tubes were wrapped in Parafilm and stored in Drierite for 3 months in darkness at room temperature and atmospheric pressure before being removed and rehydrated with laboratory grade Milli-Q water or water containing 1 mM NaF. The sample rehydrated with 1 mM NaF showed strong activation within 1 h, with no leak observed in the no-fluoride condition (Supplemental Figure S3). Interestingly, lyophilization appeared to suppress leak in the no-fluoride condition without impacting the ability to activate expression with fluoride. The maintained viability of reactions after three months indicates that storage in desiccant and light shielding to prevent catechol oxidation are the only requirements for long-term storage of

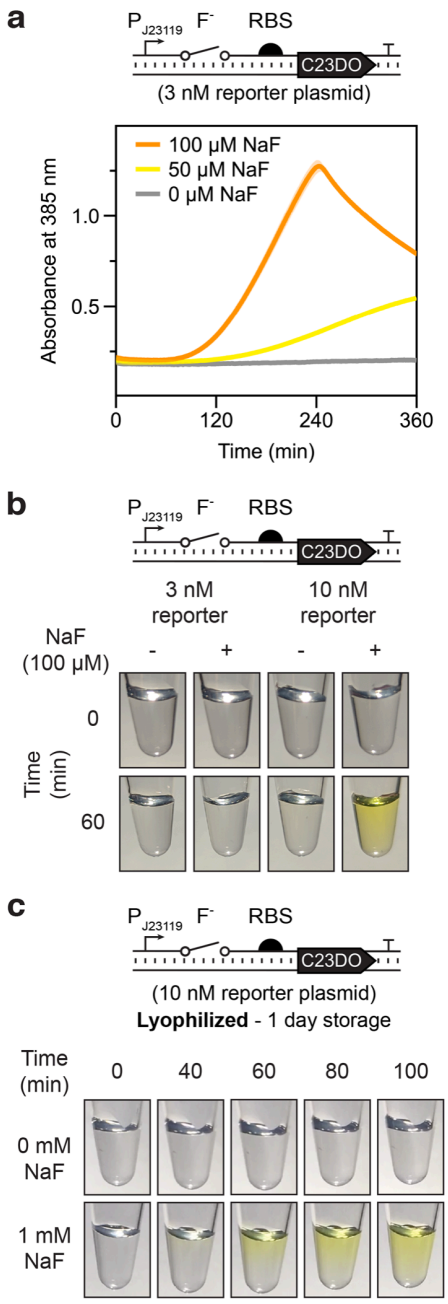

Figure 3. Colorimetric reporters enable fluoride sensing at environmentally relevant concentrations. (a) Time course of 385 nm absorbance as measured by plate reader in the presence of 100 μM NaF (orange), 50 μM NaF (yellow), and 0 μM NaF (gray) using C23DO as a reporter and incubated at 30 °C. Trajectories represent average and error shading represents one standard deviation from three technical replicates. (b) Color change observed after 1-h for two different reporter template concentrations with and without 100 μM NaF. Tubes were mixed by pipetting and incubated at 37 °C before image capture at 60 min. (c) Time lapse of rehydrated lyophilized reactions incubated at 37 °C in the absence (top) and presence (bottom) of 1 mM NaF.

DOI: 10.1021/acssynbio.9b00347
ACS Synth. Biol. 2020, 9, 10−18

lyophilized cell-free reactions, a crucial step toward field-deployment.

Point-of-Use Detection of Environmental Fluoride with a Lyophilized Biosensor. Components of environmental water samples, particularly natural ions like sodium, magnesium, or potassium, could poison cell-free reactions upon rehydration. These "matrix effects" would then impede the translation of a sensor from lab experiments to field testing and must be accounted for in a field-deployable diagnostic. To test the robustness of our system against matrix effects, we created mock fluoride-containing field samples by sampling water from a municipal tap, Lake Michigan, and an outdoor swimming pool, with Milli-Q water used as a control. NaF was then added to each sample to a final concentration of 1 mM. The biosensing reactions were prepared as before and pipetted into PCR tubes (Figure 4a, top) or spotted on BSA-treated chromatography paper (Figure 4a, bottom) before being lyophilized overnight. After lyophilization, reactions were immediately rehydrated with either unaltered mock field sample (− condition) or mock field sample containing 1 mM NaF (+ condition) and incubated at 37 °C for 1 h. For all fluoride-containing samples both in tubes and on paper, a color change was observed within 1 h, with no color development in any of the no-fluoride conditions. These results confirm that the fluoride biosensor is robust against the unfiltered environmental samples tested and can be used in real-world conditions.

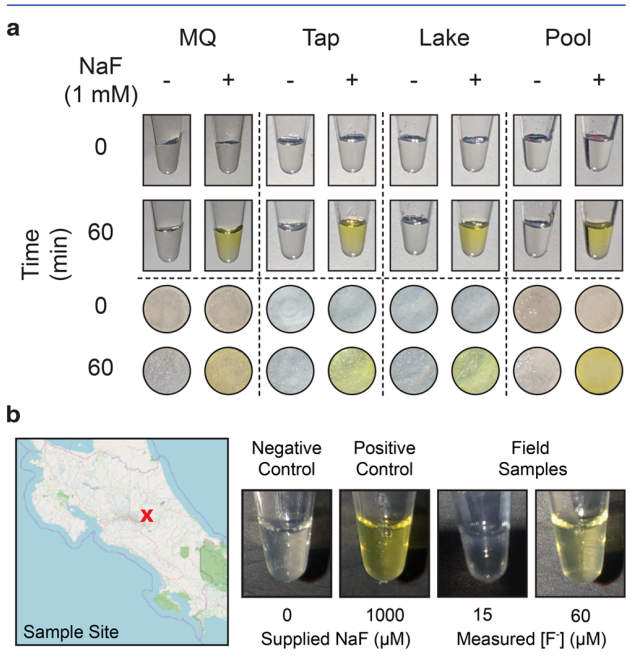

Figure 4. The cell-free fluoride riboswitch biosensor functions with real-world water samples and is not impacted by long-term storage and distribution. (a) Cell-free reactions rehydrated with various water samples with or without 1 mM NaF added. Lyophilized reactions in tubes are shown above lyophilized reactions on chromatography paper before and after 1 h incubation at 37 °C. MQ = laboratory grade Milli-Q water; Tap = tap water; Lake = unfiltered Lake Michigan water; Pool = unfiltered outdoor pool water. Uncropped photos of chromatography paper experiments are available in Supplemental Figure S8. (b) Field testing of lyophilized cell-free reactions rehydrated with water sampled in Cartago, Costa Rica. Geographical data © OpenStreetMap contributors.[22] The positive control contained 1 mM NaF in the reaction before lyophilization. The negative control was rehydrated with Milli-Q water, and the positive control and each test were rehydrated with 20 μL of unprocessed field sample followed by body-heat incubation for 5 h. Measured fluoride concentrations obtained using a fluoride sensing electrode. Field samples are from sites B and E in Supplemental Table S2.

As the culmination of our optimization process, we tested our sensor's ability to accurately classify fluoride-containing samples in the field. We specifically sought to follow a previously published environmental fluoride study that used conventional methods to sample and test publicly available natural and municipal water sources near the Irazu volcano in Cartago, Costa Rica, an area shown to have elevated fluoride levels (Supplemental Figure S4).[23] To do this, we manufactured lyophilized fluoride biosensor reactions and transported them to Costa Rica using our simplified desiccant packaging (Supplemental Figure S5A) for field testing. Sampling regions identified in the previous study,[23] we collected samples in 50 mL conical tubes and tested for fluoride in batch by adding unprocessed water to lyophilized reactions in PCR tubes *via* single-use exact volume transfer pipettes (Supplemental Figure S5B).

All field-testing was done onsite in Costa Rica without access to laboratory resources or equipment. Reactions were incubated at approximately 37 °C by being held in the armpit, with reaction time increased to 5 h to control for delayed activation caused by the imprecision of body heat incubation and low environmental fluoride concentrations.[18] A strong yellow color developed in every positive control reaction within an hour, confirming robustness to reaction poisoning by potential sample matrix effects (Supplemental Table S2). No activation was observed within 5 h in any samples with fluoride concentrations less than 50 μM (~1 ppm) as measured in cross-validation with a commercial fluoride-sensing electrode. However, a visible color change was observed after 3.5 h in a water sample collected from a roadside ditch measured to have a fluoride concentration of 60 μM (Figure 4b). This delayed activation aligns with our previous characterization in detecting trace concentrations of fluoride below 100 μM (Figure 3a). For all samples, the commercial electrode measurement confirmed the conclusions drawn from the cell-free sensors, with no false positives or false negatives observed under any conditions (n = 9) (Supplemental Table S2). By accurately detecting levels of fluoride relevant to public health concern thresholds in a real-world water source with minimal supplementary equipment, we have shown that lyophilized fluoride biosensor CFE reactions can be effectively used as low-cost, point-of-use diagnostics, demonstrating the potential of engineered biosensor elements for small molecule detection in the field.

■ DISCUSSION

In this work, we have demonstrated that a fluoride riboswitch can be implemented in a CFE system to act as a field-deployable diagnostic for environmental water samples. To the best of our knowledge, this is the first demonstration of a cell-free riboswitch-based biosensor that can detect health-relevant small molecules at regulatory levels within the field. Importantly, this work represents a significant improvement in efficacy over commercially available consumer kits (Supplemental Figure S6) and provides significant simplification and cost savings over gold standard electrochemical methods of fluoride detection, which cost hundreds to

DOI: 10.1021/acssynbio.9b00347
ACS Synth. Biol. 2020, 9, 10−18

thousands of dollars and are cumbersome to use even for scientifically skilled operators. In contrast, our biosensors can currently be made for $0.40/reaction,[20] only require a drop of water, and are robust to temperature variation, enabling incubation with body heat.

A key strength of cell-free biosensing is that biochemical parameters such as cofactor and DNA concentration can be easily tuned to reduce leak and improve dynamic range, which has been a historically difficult challenge for riboswitch engineering in cells. Furthermore, since riboswitches are *cis*-acting, only one DNA template concentration needs to be tuned per sensor, simplifying the optimization space relative to *trans*-acting RNA or protein regulators. When optimizing these reactions for the field, we found that reactions lyophilized in PCR tubes had advantages over paper-based reactions, which rapidly dried out even when incubated in sealed, humidified containers. This effect was exacerbated by the longer incubation times required for low analyte concentrations, variabilities in ambient temperature, and the practical difficulty of equipment-free incubation of paper sensors using body heat, making the tube format much more amenable to the challenges of field deployment.

This work also highlights the feasibility of using transcriptional riboswitch-mediated gene expression to convert weak-binding RNA aptamers into functional biosensors. We were surprised to find that the *B. cereus crcB* riboswitch activated so well in an *E. coli* cell-free lysate system, given the sophisticated nature of its folding mechanism and transcriptional read-through observed both *in vitro* and *in vivo*[13,24] Transcriptional riboswitches often show weak activation due to the short time scales of their regulatory decision-making, resulting in sensitivities that are kinetically, rather than thermodynamically limited.[25] Coupling transcriptional riboswitches to enzymatic outputs like C23DO can amplify weak signals, since each reporter enzyme turns over multiple molecules of substrate.[26] The combined kinetic mechanism of switching and the signal amplification afforded by a colorimetric reporter resulted in our sensor achieving a limit of detection of 50 μM, less than half of the lowest previously measured K_D for any fluoride aptamer.[27] Thus, this work is a powerful example of why considering only thermodynamic binding affinities during aptamer selection can exclude promising, diagnostically relevant sensors.

The strategies we present here could be applied to optimize the performance of a large number of natural riboswitches for the detection of metabolites and ions relevant to environmental and human health monitoring.[28] Additionally, the compatibility of CFE reactions for high-throughput screening[29] and the simple format of our DNA expression construct could be used to characterize the thousands of "orphan" riboswitches that have been bioinformatically identified but bind to unknown ligands.[30] We imagine that these strategies could even be used to re-engineer riboswitches to have novel function.[31−33] As the rules of riboswitch mechanisms are deciphered at deeper levels,[13,34−36] we hope to reach a sufficient understanding to design their functional properties to meet the global needs for field-deployable environmental and health diagnostics.

■ MATERIALS AND METHODS

Plasmid Construction. Plasmids were assembled using Gibson assembly (New England Biolabs, Cat#E2611S) and purified using a Qiagen QIAfilter Midiprep Kit (QIAGEN, Cat#12143). pJBL7025 and pJBL7026 were assembled from pJBL3752. A table of all plasmid sequences can be found in Supplemental Table S1.

Extract Preparation. Extracts were prepared according to published protocols using sonication and postlysis processing in the Rosetta2 (DE3) pLysS strain.[10] Briefly, cells are plated on a chloramphenicol-selective agar plate and incubated overnight then used to inoculate a 20 mL overnight starter culture for a 1 L final culture. This culture is grown to an optical density (OD600) of 3.0 ± 0.2 then pelleted and lysed by sonication before centrifugation for 10 min at 4 °C and 12 000*g*. After lysis, extracts were incubated with shaking for 80 min at 37 °C and 200 rpm then recentrifuged under the same conditions. The supernatant was injected into a 10K MWCO dialysis cassette (Thermo Fisher, 66380) and dialyzed at 4 °C for 3 h before a final centrifugation under the same conditions and snap-freezing in liquid nitrogen.

CFE Experiment. CFE reactions were prepared according to established protocols.[10] Briefly, reactions are composed of cell extract, a reaction buffer containing NTPs, amino acids, buffering salts, crowding agents, and an energy source, and a mix of template DNA and inducers in an approximately 30/30/40 ratio. Between reactions, the only conditions varied are DNA template and concentration, inducer concentration, and buffering magnesium glutamate concentration, the last of which is optimized by extract. Optimal magnesium glutamate concentration was 20 mM for shelf stability and field deployment experiments and 12 mM for all other data. Little variability was seen in extract performance between batches using the appropriate optimal magnesium concentrations (Supplemental Figure S7).

For an example reaction setup, refer to the Supplemental Experimental Design Spreadsheet. All kinetic CFE reactions were prepared on ice in triplicate at the 10 μL scale. 33 μL of a mixture containing the desired reaction components was prepared and then 10 μL was pipetted into three wells of a 384-well plate (Corning, 3712), taking care to avoid bubbles. Plates were sealed (Thermo Scientific, 232701) and kinetic data was monitored on a BioTek Synergy H1m plate reader for sfGFP (20 nM reporter plasmid, emission/excitation: 485/520 nm every 5 min for 8 h at 30 °C), C23DO (variable reporter plasmid concentration, 385 nm absorbance every 30 s for 4−6 h at 30 °C), and 3WJdB (20 nM reporter plasmid, emission/excitation 472/507 nm every 30 s for 2 h at 30 °C). C23DO reactions were supplemented with 1 mM catechol and 3WJdB reactions were supplemented with 20 μM DFHBI-1T. For all fluorescence experiments, a no-DNA negative control was prepared in triplicate for every extract being tested. All reported fluorescence values have been baseline-subtracted by the average of three samples from the no-DNA condition. Baseline subtraction was not performed for catechol reactions because reaction progress is determined from time to activation rather than maximal absorbance value. For the data depicted in Figure 1c, NaF and NaCl titrations were performed in separate experiments.

Mean Equivalent Fluorescence Calibration. Fluorescence measurements were calibrated to a standard curve of fluorescein isothiocyanate (FITC) fluorescence to give standardized fluorescence units of μM equivalent FITC following a previously established procedure.[37] Briefly, serial dilutions were performed from a 50 μM stock and prepared in a pH 9.5, 100 mM sodium borate buffer. Fluorescence values for these samples were read at an excitation wavelength of 485 nm and

DOI: 10.1021/acssynbio.9b00347
ACS Synth. Biol. 2020, 9, 10−18

emission wavelength of 520 nm for sfGFP and an excitation wavelength of 472 nm and emission wavelength of 507 nm for 3WJdB. These values were then used to calculate a linear conversion factor relating the plate reader's output in arbitrary units to the FITC standard curve.

Lyophilization. All lyophilization was performed in a Labconco FreeZone 2.5 Liter −84 °C Benchtop Freeze-Dryer (Cat# 710201000). A CFE reaction master mix was prepared and split into 20 μL aliquots in PCR strip tubes. Tube caps were then pierced with a pin and strips were wrapped in aluminum foil before being flash frozen in liquid nitrogen and lyophilized overnight at 0.04 mbar. After lyophilization, pierced PCR strip tube caps were replaced. Tubes were then sealed with parafilm and placed directly into Drierite (Cat#11001) for storage at room temperature (Supplemental Figure S5A).

Paper Sensors. Individual sensors were punched out of Whatman 1 CHR chromatography paper (3001−861) using a Swingline Commercial Desktop Punch (A7074020). Tickets were then placed in a Petri dish and immersed in 4% BSA for 1 h before being transferred to a new dish and left to air-dry overnight. After drying, tickets were spotted with 20 μL of CFE reaction and placed in plastic jars (QOSMEDIX 29258), which were loosely capped and wrapped in aluminum foil before being flash frozen in liquid nitrogen and lyophilized overnight at 0.04 mbar. For testing, tickets were transferred to new jars and rehydrated with 20 μL of sample solution. Jars were then closed and sealed with parafilm before incubation for 1 h at 37 °C.

Field Deployment. 20 μL lyophilized reactions were prepared with 10 nM pJBL7025 and 1 mM catechol. As a positive control, additional reactions were lyophilized after being pre-enriched with 1 mM NaF. Supplemental Table S2 contains a complete list of sample site locations and water sources tested. 50 mL water samples were collected and stored in Falcon tubes (Fisher Scientific, Cat# 14-432-22) without any processing or filtration. Reactions were rehydrated by using 20 μL exact volume transfer pipettes (Thomas Scientific, 1207F80) to pull from collected samples. Three reactions were run at each sample site: (1) a positive control rehydrated with the sample, (2) a blank reaction rehydrated with the sample, and (3) a negative control reaction rehydrated with purified water to test for any reaction leak. Reactions were placed in a plastic bag and incubated at body temperature in the armpit for 5 h using established protocols and marked as activated if a visible yellow color was observed.[18] Quantitative measurements of fluoride concentration of the same sample were taken with an Extech ExStik Waterproof Fluoride Meter (Cat# FL700). Geographical data from OpenStreetMap is licensed under the Open Data Commons Open Database License (https://www.openstreetmap.org/copyright).

Image Capture. All images were captured with *via* cell phone camera, with no specialized photography setup and no postcapture editing done aside from cropping image borders. Tubes were illuminated from below *via* desk lamp to highlight reaction color change. Paper sensors were illuminated from above *via* desk lamp and photographed without removal from the plastic jars used for incubation.

■ ASSOCIATED CONTENT

Supporting Information

The Supporting Information is available free of charge at https://pubs.acs.org/doi/10.1021/acssynbio.9b00347.

Supplemental Figures S1−S8, Supplemental Tables S1 and S2 (PDF)

Supplemental experimental design spreadsheet (XLSX)

Supplemental Video S1: Time lapse of sensor activation depicted in Figure 3c; Tubes were rehydrated with either water (left) or 1 mM NaF (right); Total time elapsed is 100 minutes (MP4)

■ AUTHOR INFORMATION

Corresponding Author

*E-mail: jblucks@northwestern.edu.

ORCID

Nancy Kelley-Loughnane: 0000-0003-2974-644X

Michael C. Jewett: 0000-0003-2948-6211

Julius B. Lucks: 0000-0002-0619-6505

Author Contributions

Conceptualization, W.T., A.D.S., M.C.J., and J.B.L.; Data Curation, W.T., A.D.S., and M.S.V.; Formal Analysis, W.T and A.D.S.; Investigation, W.T., A.D.S, and M.S.V.; Methodology, W.T., A.D.S., M.S.V., and J.B.L.; Project administration, W.T. and J.B.L.; Validation, W.T., A.D.S., and M.S.V.; Funding acquisition, N.K., M.C.J., and J.B.L.; Writing (original draft), W.T., A.D.S., and J.B.L.; Writing (review and editing), W.T., A.D.S., M.S.V., M.C.J., and J.B.L.

Notes

The authors declare the following competing financial interest(s): The authors have submitted one provisional patent application (U.S. Patent Application Serial No. 62/813,368) for the technologically important developments included in this work. J.B.L is a cofounder of Stemloop, Inc. J.B.L.s interests are reviewed and managed by Northwestern University in accordance with their conflict of interest policies. All source data for the main and SI figures were deposited open access in Northwestern's Arch database (https://arch.library.northwestern.edu). Data can be accessed *via* DOI: 10.21985/N2RJ64.

All plasmids are deposited in Addgene with accession numbers 128809−128811.

■ ACKNOWLEDGMENTS

We would like to thank Professor Ana Gabriela Calderón Cornejo (Universidad de Costa Rica) and Eduardo Quirós Morales for assistance with biosensor field-testing. We also thank Ashty Karim (Northwestern University) and Professor Robert Batey (University of Colorado, Boulder) for helpful comments in preparing the manuscript, along with Khalid Alam (Stemloop, Inc.) for editing the supplemental video, Jaeyoung Jung (Northwestern University) for assistance with designing the graphical abstract, and Professor Thomas Shahady (University of Lynchburg) for helpful comments about water sampling in Costa Rica. This work was supported by the Air Force Research Laboratory Center of Excellence for Advanced Bioprogrammable Nanomaterials (C-ABN) Grant FA8650-15-2-5518 (to M.C.J. and J.B.L), the David and Lucile Packard Foundation (to M.C.J.), an NSF CAREER Award (1452441 to J.B.L.), and the Camille Dreyfus Teacher-Scholar Program (to M.C.J. and J.B.L.). A.D.S. was supported in part by the National Institutes of Health Training Grant (T32GM008449) through Northwestern University's Biotechnology Training Program. The views and conclusions contained herein are those of the authors and should not be

DOI: 10.1021/acssynbio.9b00347
ACS Synth. Biol. 2020, 9, 10−18

interpreted as necessarily representing the official policies or endorsements, either expressed or implied, of the Air Force Research Laboratory, Air Force Office of Scientific Research, or US Government.

REFERENCES

(1) WHO (2016) *World Health Statistics 2016: Monitoring Health for the SDGs Sustainable Development Goals*, World Health Organization.

(2) Onda, K., LoBuglio, J., and Bartram, J. (2012) Global Access to Safe Water: Accounting for Water Quality and the Resulting Impact on MDG Progress. *Int. J. Environ. Res. Public Health 9* (3), 880−894.

(3) Meenakshi, and Maheshwari, R.C. (2006) Fluoride in Drinking Water and Its Removal. *J. Hazard. Mater. 137* (1), 456−463.

(4) World Health Organization (2011) Guidelines for Drinking-Water Quality. *WHO Chron. 38* (4), 104−108.

(5) Zhou, Y., Zhang, J. F., and Yoon, J. (2014) Fluorescence and Colorimetric Chemosensors for Fluoride-Ion Detection. *Chem. Rev. 114* (10), 5511−5571.

(6) Pardee, K., Green, A. A., Ferrante, T., Cameron, D. E., DaleyKeyser, A., Yin, P., and Collins, J. J. (2014) Paper-Based Synthetic Gene Networks. *Cell 159* (4), 940−954.

(7) Pardee, K., Green, A. A., Takahashi, M. K., Braff, D., Lambert, G., Lee, J. W., Ferrante, T., Ma, D., Donghia, N., Fan, M., et al. (2016) Rapid, Low-Cost Detection of Zika Virus Using Programmable Biomolecular Components. *Cell 165* (5), 1255−1266.

(8) Gräwe, A., Dreyer, A., Vornholt, T., Barteczko, U., Buchholz, L., Drews, G., Ho, U. L., Jackowski, M. E., Kracht, M., Lüders, J., et al. (2019) A Paper-Based, Cell-Free Biosensor System for the Detection of Heavy Metals and Date Rape Drugs. *PLoS One 14* (3), No. e0210940.

(9) Gupta, S., Sarkar, S., Katranidis, A., and Bhattacharya, J. (2019) Development of a Cell-Free Optical Biosensor for Detection of a Broad Range of Mercury Contaminants in Water: A Plasmid DNA-Based Approach. *ACS Omega 4* (5), 9480−9487.

(10) Silverman, A., Kelley-Loughnane, N., Lucks, J. B., and Jewett, M. C. (2019) Deconstructing Cell-Free Extract Preparation for in Vitro Activation of Transcriptional Genetic Circuitry. *ACS Synth. Biol. 8* (2), 403−414.

(11) Silverman, A. D., Karim, A. S., and Jewett, M. C. (2019) Cell-free gene expression: an expanded repertoire of applications. *Nat. Rev. Genet.*, 1.

(12) Baker, J. L., Sudarsan, N., Weinberg, Z., Roth, A., Stockbridge, R. B., and Breaker, R. R. (2012) Widespread Genetic Switches and Toxicity Resistance Proteins for Fluoride. *Science (Washington, DC, U. S.) 335* (6065), 233−235.

(13) Watters, K. E, Strobel, E. J, Yu, A. M, Lis, J. T, and Lucks, J. B (2016) Cotranscriptional Folding of a Riboswitch at Nucleotide Resolution. *Nat. Struct. Mol. Biol. 23* (12), 1124.

(14) Doull, J., Boekelheide, K., Farishian, B. G., Isaacson, R. L., Klotz, J. B., Kumar, J. V., Limeback, H., Poole, C., Puzas, J. E., and Reed, N. M. R. (2006) In *Fluoride in Drinking Water: A Scientific Review of EPA's Standards*, pp 205−223, The National Academies Press, Washington, D.C., DOI: 10.17226/11571.

(15) Zadeh, J. N., Steenberg, C. D., Bois, J. S., Wolfe, B. R., Pierce, M. B., Khan, A. R., Dirks, R. M., and Pierce, N. A. (2011) NUPACK: Analysis and Design of Nucleic Acid Systems. *J. Comput. Chem. 32* (1), 170−173.

(16) McNerney, M. P., Zhang, Y., Steppe, P., Silverman, A. D., Jewett, M. C., and Styczynski, M. P. (2019) Point-of-Care Biomarker Quantification Enabled by Sample-Specific Calibration. *Sci. Adv. 5* (9), eaax4473.

(17) Alam, K. K., Tawiah, K. D., Lichte, M. F., Porciani, D., and Burke, D. H. (2017) A Fluorescent Split Aptamer for Visualizing RNA−RNA Assembly In Vivo. *ACS Synth. Biol. 6* (9), 1710−1721.

(18) Verosloff, M., Chappell, J., Perry, K. L., Thompson, J. R., and Lucks, J. B. (2019) PLANT-Dx: A Molecular Diagnostic for Point-of-Use Detection of Plant Pathogens. *ACS Synth. Biol. 8* (4), 902−905.

(19) Chappell, J., Westbrook, A., Verosloff, M., and Lucks, J. B. (2017) Computational Design of Small Transcription Activating RNAs for Versatile and Dynamic Gene Regulation. *Nat. Commun. 8* (1), 1051.

(20) Stark, J. C., Huang, A., Nguyen, P. Q., Dubner, R. S., Hsu, K. J., Ferrante, T. C., Anderson, M., Kanapskyte, A., Mucha, Q., Packett, J. S., et al. (2018) BioBits™ Bright: A Fluorescent Synthetic Biology Education Kit. *Sci. Adv. 4* (8), eaat5107.

(21) Huang, A., Nguyen, P. Q., Stark, J. C., Takahashi, M. K., Donghia, N., Ferrante, T., Dy, A. J., Hsu, K. J., Dubner, R. S., Pardee, K., et al. (2018) BioBits™ Explorer: A Modular Synthetic Biology Education Kit. *Sci. Adv. 4* (8), eaat5105.

(22) Haklay, M., and Weber, P. (2008) Openstreetmap: User-Generated Street Maps. *Ieee Pervas Comput 7* (4), 12−18.

(23) Rojas Zuniga, F., Floor, G., Malavassi, E., Martinez Cruz, M., and Van Bergen, M. (2014) Fluorosis Dental En La Población Infantil En Las Cercanias Del Volcán Irazú, Costa Rica. *Congr. Latinoam. Estud. Química Paraguay*.

(24) Zhao, B., Guffy, S. L., Williams, B., and Zhang, Q. (2017) An Excited State Underlies Gene Regulation of a Transcriptional Riboswitch. *Nat. Chem. Biol. 13* (9), 968−974.

(25) Wickiser, J. K., Winkler, W. C., Breaker, R. R., and Crothers, D. M. (2005) The Speed of RNA Transcription and Metabolite Binding Kinetics Operate an FMN Riboswitch. *Mol. Cell 18* (1), 49−60.

(26) Karzbrun, E., Shin, J., Bar-Ziv, R. H., and Noireaux, V. (2011) Coarse-Grained Dynamics of Protein Synthesis in a Cell-Free System. *Phys. Rev. Lett. 106* (4), 48104.

(27) Ren, A., Rajashankar, K. R., and Patel, D. J. (2012) Fluoride Ion Encapsulation by Mg 2+ Ions and Phosphates in a Fluoride Riboswitch. *Nature 486* (7401), 85.

(28) McCown, P. J., Corbino, K. A., Stav, S., Sherlock, M. E., and Breaker, R. R. (2017) Riboswitch Diversity and Distribution. *RNA 23* (7), 995−1011.

(29) Moore, S. J., MacDonald, J. T., Wienecke, S., Ishwarbhai, A., Tsipa, A., Aw, R., Kylilis, N., Bell, D. J., McClymont, D. W., Jensen, K., et al. (2018) Rapid Acquisition and Model-Based Analysis of Cell-Free Transcription−Translation Reactions from Nonmodel Bacteria. *Proc. Natl. Acad. Sci. U. S. A. 115* (19), E4340.

(30) Greenlee, E. B., Stav, S., Atilho, R. M., Brewer, K. I., Harris, K. A., Malkowski, S. N., Mirihana Arachchilage, G., Perkins, K. R., Sherlock, M. E., and Breaker, R. R. (2018) Challenges of Ligand Identification for the Second Wave of Orphan Riboswitch Candidates. *RNA Biol. 15* (3), 377−390.

(31) Boussebayle, A., Torka, D., Ollivaud, S., Braun, J., Bofill-Bosch, C., Dombrowski, M., Groher, F., Hamacher, K., and Suess, B. (2019) Next-Level Riboswitch Development—Implementation of Capture-SELEX Facilitates Identification of a New Synthetic Riboswitch. *Nucleic Acids Res. 47* (9), 4883−4895.

(32) Espah Borujeni, A., Mishler, D. M., Wang, J., Huso, W., and Salis, H. M. (2016) Automated Physics-Based Design of Synthetic Riboswitches from Diverse RNA Aptamers. *Nucleic Acids Res. 44* (1), 1−13.

(33) Wu, M. J., Andreasson, J. O. L., Kladwang, W., Greenleaf, W. J., and Das, R. (2019) Automated Design of Diverse Stand-Alone Riboswitches. *ACS Synth. Biol. 8* (8), 1838−1846.

(34) Frieda, K. L., and Block, S. M. (2012) Direct Observation of Cotranscriptional Folding in an Adenine Riboswitch. *Science (Washington, DC, U. S.) 338* (6105), 397−400.

(35) Drogalis, L. K., and Batey, R. T. (2018) Requirements for Efficient Cotranscriptional Regulatory Switching in Designed Variants of the *Bacillus subtilis* PbuE Adenine-Responsive Riboswitch. *bioRxiv*, DOI: 10.1101/372573.

(36) Strobel, E. J., Cheng, L., Berman, K. E., Carlson, P. D., and Lucks, J. B. (2019) A Ligand-Gated Strand Displacement Mechanism for ZTP Riboswitch Transcription Control. *Nat. Chem. Biol. 15* (11), 1067−1076.

(37) Alam, K. K., Jung, J. K., Verosloff, M. S., Clauer, P. R., Lee, J. W., Capdevila, D. A., Pastén, P. A., Giedroc, D. P., Collins, J. J., and Lucks, J. B. (2019) Rapid, Low-Cost Detection of Water

DOI: 10.1021/acssynbio.9b00347
ACS Synth. Biol. 2020, 9, 10−18

Contaminants Using Regulated *In Vitro* Transcription. *bioRxiv*, DOI: 10.1101/619296.

DOI: 10.1021/acssynbio.9b00347
ACS Synth. Biol. 2020, 9, 10−18